Predicting potential habitat distribution of the invasive species *Rhynchophorus ferrugineus* Olivier in China based on MaxEnt modelling technique and future climate change

Zhiling Wang[1,*], Zhihang Zhuo[1,*], Habib Ali[2], Sumbul Mureed[3], Quanwei Liu[1], Xuebin Yang[1] and Danping Xu[1] (ID)

[1]College of Life Science, China West Normal University, Nanchong 637002, China; [2]Depatment of Agricultural Engineering, Khwaja Fareed University of Engineering and Information Technology, Rahim Yar Khan 64200, Pakistan and [3]College of Forestry, Sichuan Agricultural University, Chengdu 611130, China

Abstract

Changes in the distribution of species due to global climate change have a critically significant impact on the increase in the spread of invasive species. An in-depth study of the distribution patterns of invasive species and the factors influencing them can help to better predict and combat invasive alien species. *Rhynchophorus ferrugineus* Olivier is an invasive species that primarily harms plants of *Trachycarpus* H. Wendl. The pest invades trees in three main ways: by laying eggs and incubating them in the crown of the plant, on roots at the surface and at the base of the trunk or petiole. Most of the plants in the genus *Trachycarpus* are taller, and the damage is concentrated in the middle and upper parts of the plant, making control more difficult. In this paper, we combine 19 bioclimatic variables based on the MaxEnt model to project the current and future distributions of *R. ferrugineus* under three typical emission scenarios (2.6 W m^{-2} (SSP1-2.6), 4.5 W m^{-2} (SSP2-4.5) and 8.5 W m^{-2} (SSP5-8.5)) in the 2050s and 2090s. Among the 19 bioclimatic variables, five variables were screened out by contribution rates, namely annual mean temperature (BIO 1), precipitation of driest quarter (BIO 17), minimum temperature of coldest month (BIO 6), mean diurnal range (BIO 2) and precipitation of wettest quarter (BIO 16). These five variables are key environmental variables that influence habitat suitability for *R. ferrugineus* and are representative in reflecting its potential habitat. The results showed that *R. ferrugineus* is now widely distributed in the southeastern coastal area of China (high suitability zone), concentrating in the provinces of Hainan, Guangdong, Fujian, Guangxi and Taiwan. In the future, the area of high and low suitability zones will increase and the area of medium suitability zones will decrease. The area of low suitability zone will still be in the largest proportion. This study aims to provide a theoretical reference for the future control of *R. ferrugineus* from the perspective of geographic distribution.

Introduction

Rhynchophorus ferrugineus Olivier, also known as the red palm weevil (RPW), belongs to the family Coleoptera, Curculionidae (Ahmed and Freed, 2021). The RPW is an invasive pest that has become fully entrenched in more than 60 countries around the world, and was first discovered in the Arabian Gulf region in the mid-1980s (Kurdi *et al.*, 2021; Yasin *et al.*, 2021). This pest originated in southern and southeastern Asia, such as India, Indonesia and Pakistan, and later spread to the Near East and North Africa. Subsequently, the RPW invaded several Middle Eastern countries, such as Iran, Iraq, Saudi Arabia, the UAE and Egypt (El-Zoghby *et al.*, 2022). In 1990, RPW was also reported in China. Since the 1980s, its geographic distribution in China has expanded rapidly. RPW monitoring was conducted in Taiwan in 1997 and severely damaged ornamental palm saplings were found in central Taiwan (Kurdi *et al.*, 2021). RPW poses a significant threat to *Trachycarpus* H. Wendl. plants. It is worth noting that RPW primarily targets palm trees within this plant category. Furthermore, the pest exhibits a preference for the economic crops of these plants.

Trachycarpus is mostly used in landscaping because of its adaptable and aesthetically pleasing plant form, as well as its resistance to a variety of toxic gases (Nengjie, 2022). In addition to this, *Trachycarpus* has some economic value. Its skin fibres, young leaves and the dark brown leaf sheaths covering the stems can be made into a variety of fibre products with excellent properties (Zhu *et al.*, 2019). At the same time, the plants of the genus have some medicinal value (Zhijun, 1998), and the RPW is one of the most dangerous and destructive of the pests that afflict *Trachycarpus* (Alshammari *et al.*, 2022; Montiel *et al.*, 2022). It is most damaging to

young *Trachycarpus* plants less than 10 years old, and generally less damaging to older trees over 30 years old. These include *Phoenix sylvestris* (L.) Roxb. (silver date palm), *P. canariensis* Chabaud (Canary Island date palm) and *Bismarckia nobilis* Hildebr. & H. Wendl. (Bismarck palms) (Kurdi *et al*., 2021). RPW is highly adapted to host plants; at least 24 species of *Trachycarpus* plants have been reported (Yang *et al*., 2023), mainly including coconut, sugar, oil, sago, palmyra, royal, Washingtonian and date palms (Kurdi *et al*., 2021). The number of hosts for the RPW has increased significantly over the past few decades (Abdel Raheem *et al*., 2020). This increase in host range is a result of its rapid geographic expansion, which is likely to continue in the future due to climate change (Montiel *et al*., 2022). This insect has now spread to palm tree plantations in southern China, causing serious damage to the palm tree industry and landscape. Special emphasis is placed on the fact that RPW is characterised by high reproductive capacity, wide range of parasitic plants, difficulty in control, high lethality, easy to concentrate outbreaks, etc., and the damage to plants is often irreversible (Abdelsalam *et al*., 2020). The RPW usually invades in the following three ways. The first, which is the most common, is the infestation of plants by adults laying eggs that hatch in wounds, fissures and cracks at the base of the trunk or petiole, and by larvae that bore into the young tissue at the base of the plant's petiole and within the trunk. The affected plants initially show slight cracking of the bark or petioles, followed by gradual yellowing and withering of the leaf margins, which then extends towards the middle of the leaves. As the damage progresses to later stages, the cores and leaves of the plants will dry up and become brittle, while their fibrous tissues undergo transformation into humus, resulting in fragmentation. Some palm plants may expel fibre crumbs or release a brown viscous liquid (commonly known as tree gum) from wormholes. When found, the affected plants are often unsalvageable, often causing the entire plant to break or die outright. The second type infiltrates the tree through surface-level roots. Affected plants exhibit reduced foliage, with certain branches and leaves wilting or drooping, while other areas appear indistinguishable from healthy plants. However, all internal tissues of the trunk are thoroughly compromised. The third type of invasion is from the crown of the tree, where the heart and leaves will all die, and this is the most damaging because the growing points quickly become necrotic. Regardless of the method of invasion, once RPW has penetrated the tree, it can usually kill the plant within 5–6 months (Abdel-Raheem *et al*., 2019).

Due to the robust reproductive capacity of RPW, failure to control it can lead to substantial ecological, environmental and economic consequences. Annually, hundreds of thousands of infected palm trees perish, directly impacting farmers' income sources. Furthermore, the demise of palm trees can result in adverse effects on the local ecological environment, such as soil erosion and diminished biodiversity, consequently impeding the development of ecotourism and associated industries (Alshammari *et al*., 2022). In China, it is one of the 233 dangerous pests of forestry announced by the State Forestry Administration of China in 2003, and is included in China's list of imported phytosanitary pests and the list of quarantine pests of agriculture and forestry (Lijiao and Yihang, 2022). The larvae of RPW are long-lived, have a strong drilling ability and are adaptable to different environments. The larval stage is the most critical stage for control, as the destruction of vascular tissues by RPW larvae and the massive consumption of canopy tissues can lead to the death of palm trees (Zhang *et al*., 2020). Biological control, such as the use of natural enemies like larval parasitic wasps (*Scolia erratica*) and adult flies (*Sarcophaga fuscicauda*), can be considered an effective means of control. Nevertheless, although natural enemies of RPW have been reported in several countries, none of them have been used as biological control due to the protected internal environment in which RPW larvae live (Yang *et al*., 2023). As it stands, the distribution of RPW is primarily concentrated along the southeastern coastal regions of China. This area also happens to be the most severely affected by the pest. When contemplating alterations in species distribution, climate stands out as the pivotal factor. Existing research has underscored the significant influence of climate on the distribution of this pest. Specifically, rising temperatures may lead to an expansion of its ecological niche (Fiaboe *et al*., 2012; Ge *et al*., 2015). So predicting the future trend of RPW's geographic distribution provides a key intervention point for preventing its expansion.

Since the 1980s, a variety of species distribution models (SDMs), also known as ecological niche models (ENMs), have been developed, which are an important tool for studying the fitness of species (Booth *et al*., 2014). The main models used for developmental prediction work include Domain Model, Ecological Niche Factor Analysis (ENFA), the Bioclimatic Prediction System (Bioclim), genetic algorithm for rule set production (GARP) and maximum entropy models (MaxEnt) (Harte *et al*., 2021; Wang *et al*., 2021; Losada *et al*., 2022; Ahmadi *et al*., 2023). The principle of SDM is to relate known locations of species to the environmental characteristics of those locations in order to estimate the response function and contribution of environmental variables, and to estimate the ecological niche of the species according to a specific algorithm (Zhou *et al*., 2021). Insights into ecological or evolutionary drivers in this way can help predict habitat suitability at large scales (Fourcade *et al*., 2014). It is worth mentioning that MaxEnt in SDMs has been increasingly adopted (Korbel, 2021). When MaxEnt is used to estimate the ecological niche and potential geographic distribution of a species, only species occurrence records and background samples of the environmental conditions in the area of interest are required. This type of data is referred to as 'presence background' (PB) data. MaxEnt applies the principle of 'maximum entropy' to fit the model to estimate the minimum extent to which the distribution of species deviates from a uniform distribution in order to explain the observations (Guillera-Arroita *et al*., 2014). MaxEnt is the most widely used SDM algorithm due to its ease of use and is believed to produce robust results with sparse data, irregular sampling and small localisation errors (Harte *et al*., 2021). The advantage of MaxEnt is that it requires the use of only a small amount of existing data, so there is no reliance on or need for specific regions to identify data that do not exist (West *et al*., 2016). Overall, these features have led MaxEnt to be considered one of the best models for predicting species distributions, especially for species that are difficult to systematically enumerate or have limited ranges (Kramer-Schadt *et al*., 2013).

In this paper, the geographic distribution of the species was collected based on the MaxEnt model and linked to 19 bioclimatic variables, analysing the importance of each variable. Several key variables that are decisive for predicting the future distribution of the species were identified. The aim was to assess the current and potential future distribution of the pest in its Chinese range and to explore the key environmental factors influencing the distribution of the pest. This will provide some references for future control of this pest.

Material and methods

Collection of occurrence data

RPW distribution point data were obtained by querying the databases of the European and Mediterranean Plant Protection Organization (EPPO, https://gd.eppo.int, accessed on 21 March 2023) and the Global Biodiversity Information Facility (GBIF, http://www.gbif.org, accessed on 22 March 2023). In addition to the online databases, distribution point data for the actual survey were obtained from relevant literature in CNKI and Web of Science. The latitude and longitude information was obtained from the geographic coordinate information provided in the literature. For records missing latitude and longitude information, Google Earth (http://ditu.google.cn) was used to obtain latitude and longitude using county location descriptions. Occurrence records without accurate location information were excluded from the database. All records are scrutinised to remove duplicate points and points without correct information. For the MaxEnt model, the distribution point data were saved in 'CSV' format. To prevent overfitting, this study employed ENMTools version 1.0.4 on the R platform to spatially filter the data based on longitude, ensuring the presence of only one distribution point per grid cell. The spatial resolution was set at 2.5 arc minutes (approximately 4.5 km). In the end, a total of 222 RPW distribution points were acquired, and their distribution is depicted in fig. S1.

Environmental variables and data processing

The environmental variables are current and future data obtained from the WorldClim Global Climate Database (http://www.worldclim.org/) and include 19 bioclimatic variables as well as 48 monthly climate variables. Current climate conditions are expressed using monthly average data from 1950 to 2000. Three representative gas emission scenarios of 2.6 W m^{-2} (SSP1-2.6), 4.5 W m^{-2} (SSP2-4.5) and 8.5 W m^{-2} (SSP5-8.5) from the Shared Economy Pathway of the Sixth International Coupled Models Intercomparison Program (CMIP6) model were selected for the future climate scenario data. These scenarios were proposed by the IPCC, and respectively they represent a stabilisation of radiative forcing by 2100 in these scenarios. Future climate data were downloaded from the International Center for Tropical Agriculture (CIAT) and generated from the second generation of the National Climate Center Moderate Resolution Climate System Model (BCC-CSM2-MR). This model is more reliable in simulating precipitation and temperature in China, and it is the latest medium-resolution climate system model developed by the National Climate Center of China (Fredriksen *et al.*, 2023). The above data, with a spatial resolution of 2.5 arc-minutes (approximately 4.5 km^2), were used to predict the distribution of potential suitability of the RPW for two periods: the 2050s (2041–2060) and the 2090s (2081–2100).

This study utilises the Jackknife test in MaxEnt to determine the extent to which each environmental variable contributes to the model construction, thereby eliminating variables that contribute less. Pearson's correlation coefficient is commonly used to determine the correlation between each pair of variables ($|r| \geq 0.8$). There are some effects on ENM predictions due to correlation and multicollinearity between climate factors. Highly correlated variables ($|r| \geq 0.8$) were removed in order to increase the accuracy of the model and minimise the effects of overfitting. Multicollinearity was detected using ENMTools (version 1.0.40). Finally, five key environment variables (BIO 1, BIO 2, BIO 6, BIO 16, BIO 17) were kept.

MaxEnt model optimisation and accuracy evaluation

In the MaxEnt model, improper selection of optimal parameters can negatively affect the prediction results, and the complexity of MaxEnt has a significant impact on the transferability of species predictions in the model (Alsamadisi *et al.*, 2020). There are two key parameters present in MaxEnt model to optimise the final model viz: feature combination (FC) and regulation multiplier (RM). These two key parameters are crucial for effectively avoiding overfitting and significantly improving the model's prediction accuracy (Barber *et al.*, 2022). Consequently, in this paper, the complexity of the model is controlled by adding parameters to the ENMTools function to regularise the model. We imported the distribution data of RPW and 19 environmental variables into MaxEnt and set the parameters to the optimal combination. Meanwhile, the receiver operating characteristic curve (ROC) is plotted to evaluate the model fit. Refer to fig. S2 for the above process.

The area under curve (AUC) of the ROC curve is used to evaluate the quality of the model results. The AUC values are independent of the critical values in the model and can be used to assess the accuracy of the model. AUC ranges from 0 to 1, with 0–0.6 indicating very poor predictive performance, 0.7–0.8 indicating fair predictive performance, 0.8–0.9 indicating good predictive performance and 0.9–1.0 indicating excellent predictive performance (Wang *et al.*, 2023). Overall, the closer the value is to 1, the better the model fit.

Delineation of potentially suitable areas

In this study, the ASC file output from MaxEnt is imported into GIS, converted into grid data and superimposed on a map of Chinese administrative divisions for visualisation. Seventy-five per cent of the distribution records were used as a randomised training dataset to build the predictive model, and 25% of the remaining distribution records were used as a test dataset, repeating this operation ten times. On this basis, the reclassification function of GIS was utilised to classify the RPW fitness zones into different areas, and the corresponding area calculations were carried out using the grid calculation tool. In this work, the distribution values were classified according to the method of assessing probability in the IPCC report, and based on the suitability index P, the suitability areas were categorised into four classes: high suitability areas ($P \geq 0.66$), medium suitability areas ($0.33 \leq P < 0.66$), low suitability areas ($0.05 \leq P < 0.33$) and unsuitable areas ($P < 0.05$) (Wang *et al.*, 2023).

Results

MaxEnt performance and the importance of environment variables

Figure 1 shows AUC with ten replications of the model. The mean test AUC value for its repeated runs was as high as 0.965 with a standard deviation of 0.012. The training AUC and test AUC were 0.967 and 0.964, respectively (table S1). Based on the previously mentioned evaluation criteria, it indicates that the model exhibits excellent predictive performance. AUC values exceeding 0.9 suggest that the model possesses high predictive accuracy.

The potential distribution of RPW under current climatic conditions was analysed using MaxEnt to model the variables selected for the study. This study was conducted by taking 19 climatic variables into account and then filtering out a few variables that
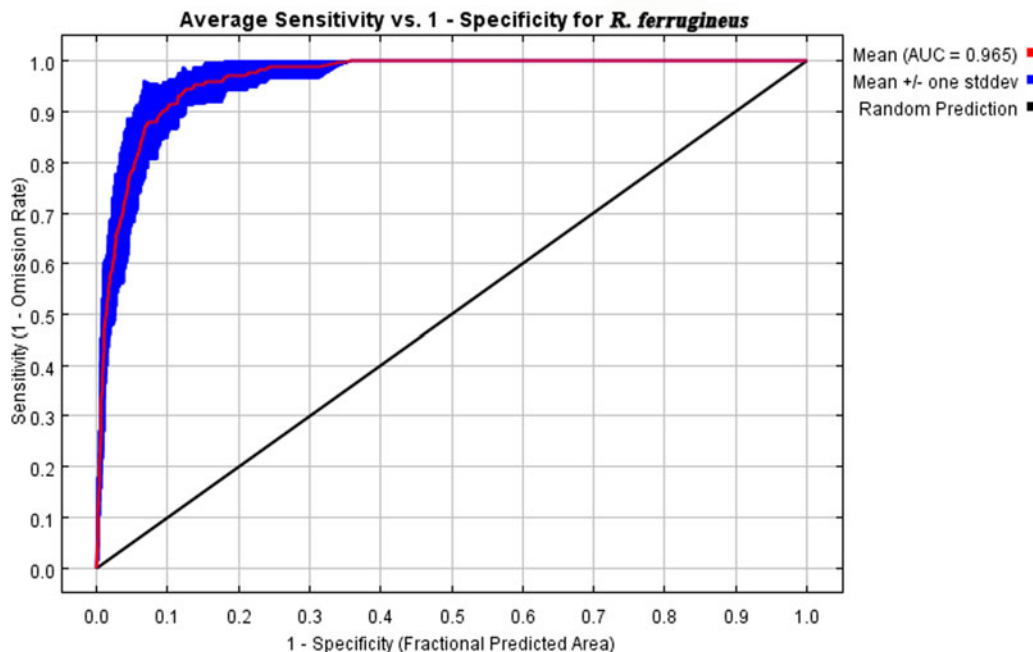
Figure 1. AUC result of MaxEnt modelling.

are determinative of the impact of RPW. Jackknife test is shown in fig. 2. Minimum temperature of coldest month (BIO 6) provides the highest gain when used independently. The next largest contribution to the model is the annual mean temperature (BIO 1). The values shown in the graph are the average of repeated runs. Under current climatic conditions, these two environmental factors had the greatest effect on RPW growth suitability, suggesting that these factors themselves contain more useful information than the other variables. As can be seen from table 1, among the five environmental variables screened by MaxEnt, BIO 1 and BIO 17 have the highest contributions of 51.3% and 31.5%, respectively. The cumulative contribution of these two environmental factors to the RPW was 82.8%. The top three contributing bioclimatic variables were BIO 1, BIO 17 and BIO 6, with the cumulative value of the three reaching 93.80%. Therefore, BIO 1, BIO 17 and BIO 6 are the primary environmental variables that influence habitat suitability for RPW and respond well to potential habitat for RPW.

Species response and potential habitat suitability distribution

Figure 3 shows the response curves for the relationship between the probability of RPW presence and the five bioclimatic variables. The figure reflects the dependence of predictive appropriateness on the selected variables, as well as the dependence caused by correlations between the selected variables and other variables. The values shown in the graph are the average of ten repetitive runs. Based on the BIO 1 curve, it can be concluded that the interval of the yearly average temperature (BIO 1) is most suitable for the survival of RPW when it ranges from 24.6 to 29.4°C. In terms of the mean diurnal temperature difference (BIO 2), there was a consistently high response between 2.80 and 5.50°C, with a sharp downward trend starting at temperatures above 5.5°C, and the insect was no longer likely to survive once above 12°C. The minimum temperature of the coldest month (BIO 6) shows an increasing trend from −3.0°C, and stabilises to reach the optimal value after reaching 15.8°C, with its optimal
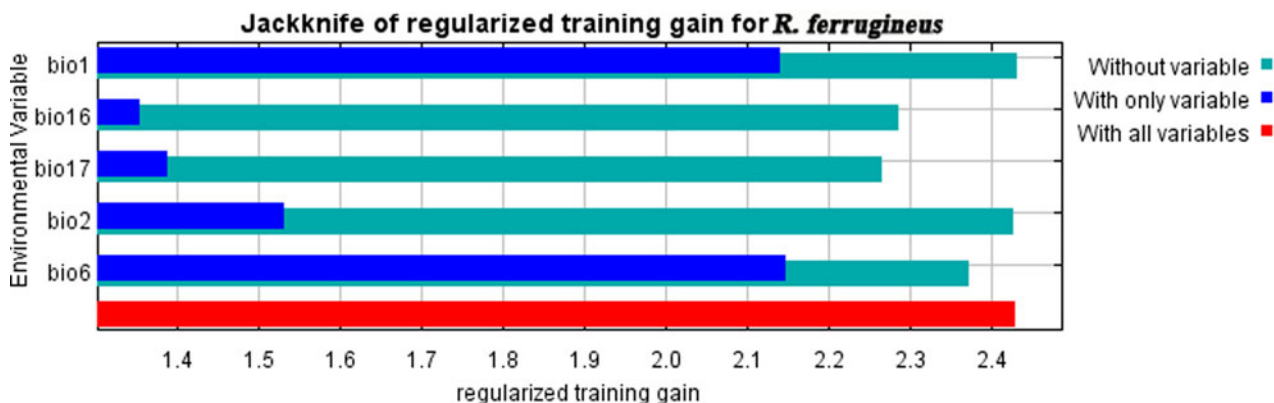

Figure 2. Jackknife plot of the training gain for *R. ferrugineus*.

Table 1. Environmental variables used in this study and their percentage contribution (%) to variation in the data

The contribution of each environmental variable in MaxEnt modelling	
Code	Per cent contribution/%
BIO 1 (annual mean temperature)	51.3
BIO 17 (precipitation of driest quarter (mm))	31.5
BIO 6 (minimum temperature of coldest month (°C))	11
BIO 2 mean diurnal range (mean of monthly (max temp–min temp) (°C))	3.6
BIO 16 precipitation of wettest quarter (mm)	2.7

interval ranging from 15.8 to 23.2°C. From fig. 3d, it can be seen that the suitability of RPW firstly shows an increasing trend with the increase of the amount of precipitation (BIO 16) in the wettest season, and then starts to decrease after the peak at 755 mm, and then the suitability tends to stabilise when it reaches 2200 mm. Precipitation in the driest quarter (BIO 17) peaks at 80 mm. It shows that RPW is positively correlated with suitability for precipitation in the driest quarter (BIO 17) below 80 mm, but negatively correlated with suitability above 80 mm. It is worth noting that it stops falling at 550 mm and shows a flat trend. The results showed that the suitability of RPW was greatest when the average annual temperature (BIO 1) ranged from 24.6 to 29.4°C, the average diurnal temperature difference (BIO 2) ranged from 2.80 to 5.50°C, the minimum temperature of the coldest month (BIO 6) ranged from 15.8 to 23.2°C, and the precipitation of the wettest season (BIO 16) was 755 mm, and the precipitation of the driest season (BIO 17) was 80 mm.

Figure 4 shows the distribution of the suitability zones of the contemporary RPW. The insect is distributed throughout the southeastern region, but the high suitability zone is mainly concentrated in the southeastern coastal region. The conditions for the formation of a monsoon climate are provided by the combined effect of warm and humid air currents from the oceans and dry and cold air currents from the continents; and because the southeastern part of China is in the tropics and subtropics, the climate type is mainly tropical monsoon climate or subtropical monsoon climate. Tropical monsoon climates have high temperatures throughout the year with distinct dry and rainy seasons for precipitation, while subtropical monsoon climates are at lower latitudes, and winters are milder rather than colder. Such climatic conditions are also exactly what the RPW needs.

Highly suitable areas are mainly located in Hainan, Guangdong, Fujian, Zhejiang, Guangxi, Taiwan and Yunnan provinces. Tables 2 and 3 show that the total area of highly suitable areas for RPW is currently $9.12 \times 10^4 \, km^2$, accounting for 1.0% of the area of China. Guangdong has the largest area of highly suitable areas, $3.06 \times 10^4 \, km^2$, accounting for 33.6% of the total area of highly suitable areas in the country. Overall, the proportionate area of high suitability zones is relatively small, with more areas in medium and low suitability zones.

Current and future distribution projections and changes

This paper focuses on the distributional trends of RPW from two future periods, the 2050s and the 2090s, and three scenarios,

SSP1-2.6, SSP2-4.5 and SSP5-8.5. The potential distribution hierarchy of RPW under the corresponding scenarios is also plotted (fig. 5), which clearly presents the future potential distribution changes of the beetle. For the high suitability area, the overall trend shows the same direction in both the 2050s and 2090s periods. The area decreases to varying degrees in both the SSP1-2.6 and SSP2-4.5 scenarios, while the increase is relatively large in both the SSP5-8.5 scenario. Under the 2050s SSP1-2.6, SSP2-4.5 and SSP5-8.5 scenarios, the RPW high suitability zones were 8.90×10^4, 8.66×10^4 and $13.51 \times 10^4 \, km^2$ respectively; under the 2090s SSP1-2.6, SSP2-4.5 and SSP5-8.5 scenarios, the RPW high suitability zones were 7.51×10^4, 8.75×10^4 and $11.05 \times 10^4 \, km^2$ respectively. The results show that the area of the high suitability zone shows an overall increasing trend. However, there is a general decrease in the area of medium suitability zones. The most significant decrease is −24.3% for the SSP5-8.5 scenario in the 2050s. In the future, the area of low suitability zones will continue to increase. Only in the 2090s did the SSP1-2.6 scenario show a small reduction in the area of low suitability zones. It is worth noting that while the high suitability district had the largest increase, the district originally had a relatively small overall area. So the high suitability zone is still much smaller than the low suitability zone, which is itself the largest. Overall, in the future, there will be an increase in the area of high and low suitability zones and a decrease in the area of medium suitability zones. The low suitability zone will continue to occupy the largest area.

Discussion

Predicting suitable habitats through SDMs has become an effective tool for invasive pest habitat suitability evaluation and pest control (Costa *et al.*, 2015). Hence, using climate change under different scenarios as an entry point to explore the possibility of future distribution of RPW is crucial for the control of this pest. In this study, MaxEnt was used to simulate a suitable habitat for RPW under current and future climate scenarios. Environmental variables have an impact on the accuracy of the model during the modelling process (Bowler, 2014). So, in this paper, the environmental variables are filtered. In parallel, the sample size of the species occurrence data also has an impact on the predictive performance of the model during the analysis process (Halvorsen *et al.*, 2016). It is shown that the analysis of different training samples regarding the reliability of the results leads to the conclusion that when the number of training samples reaches 20, the accuracy of the model basically meets the requirements. When the number of samples is greater than 30, MaxEnt will provide stable prediction results (Gao *et al.*, 2023). In this study, a total of 222 training samples of RPW occurrence were used after screening, which provided a base guarantee for the accuracy of the prediction results (AUC = 0.965). Due to the greater significance of climate change in influencing species distribution, this article primarily focuses on discussing the current and future distribution of the pest from a climatic perspective. However, the distribution of a species is not solely dictated by climate; rather, it is shaped by the interplay of abiotic and biotic factors. Incorporating more factors into modelling considerations can enhance the accuracy of predictive outcomes. This direction is worth emphasising in future forecasting efforts.

Most of the highly suitable habitats for RPW are located in the hilly areas along the southeast coast of China. Among them, Taiwan Island and Hainan Island are the first and second largest
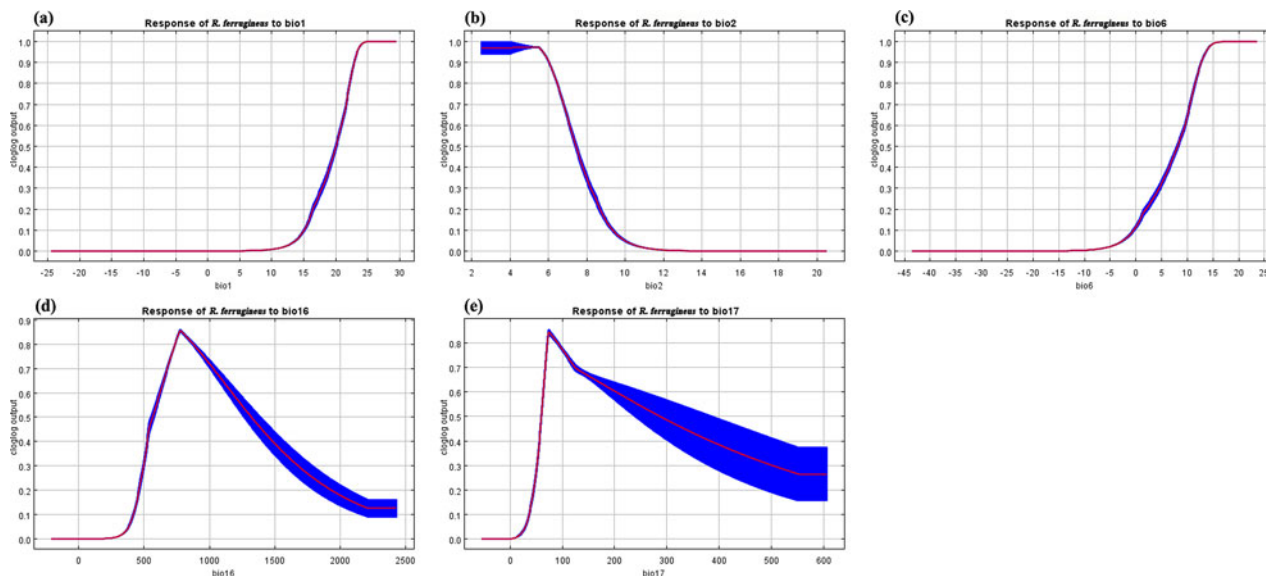
Figure 3. Response curves of the environmental variables that contributed the most to the MaxEnt models. (A) Annual mean temperature (BIO 1). (B) Mean diurnal range (mean of monthly (max temp–min temp) (°C)) (BIO 2). (C) Minimum temperature of coldest month (BIO 6). (D) Precipitation of wettest quarter (mm) (BIO 16). (E) Precipitation of driest quarter (mm) (BIO 17). The red line is the average response of the MaxEnt run. The blue part is the average±one standard deviation.

islands in China, respectively, and the four sides of the sea as well as the distribution of hills are the main reasons why the whole island of these two islands belongs to the medium- and high-suitable habitats. It is worth noting that Hainan Island, with 76% of the island's highly suitable habitat area, should be a priority control area. The plains of the middle and lower reaches of the Yangtze River are the northernmost boundary between the unsuitable area and the low, medium and high suitable habitat areas. To the north of this boundary are the North China Plain, the second largest plain in China, and the Northeast China Plain, the first largest plain in China, both of which are in unsuitable areas. The insect prefers to survive in hilly areas. This
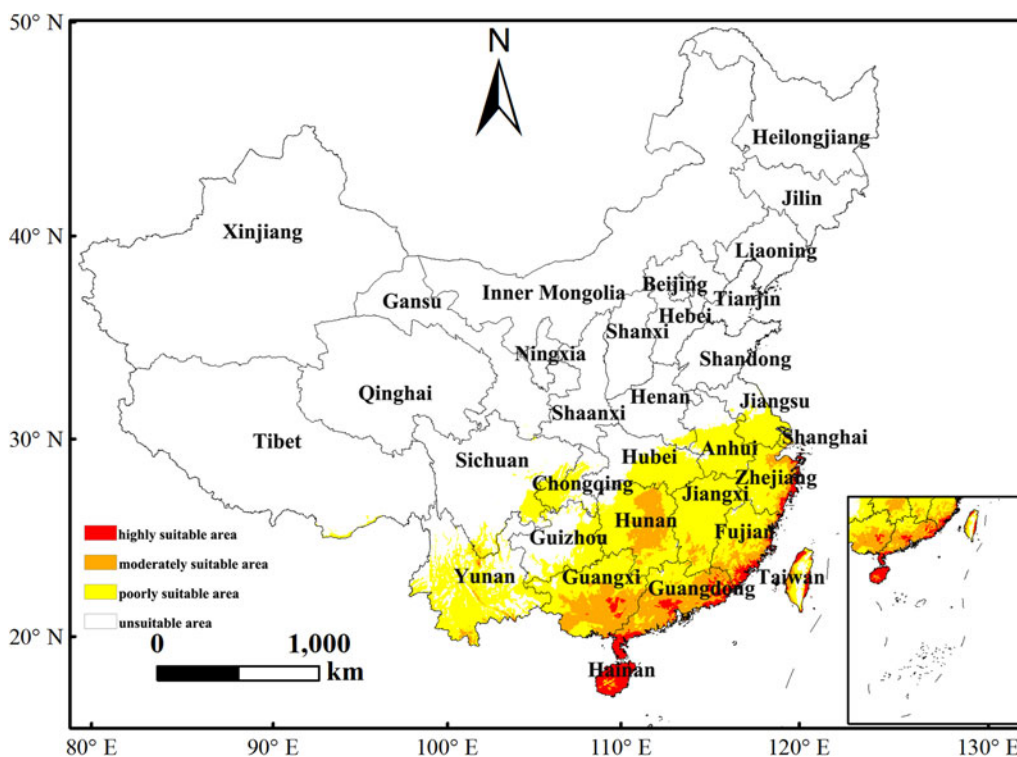

Figure 4. Current suitable climatic distribution of *R. ferrugineus* in China. The probability of *R. ferrugineus* is shown by the colour scale in the area. Red indicates a highly suitable area with a probability of higher than 0.66, orange indicates a moderately suitable area with a probability of 0.33–0.66, yellow indicates a poorly suitable area with a probability ranging from 0.05 to 0.33, and white represents unsuitable areas.

Table 2. Analysis of the main suitable distributions of *R. ferrugineus* in China

Province	High-suitable area (10^4 km²)	Moderate-suitable area (10^4 km²)	Low-suitable area (10^4 km²)	Total (10^4 km²)[a]	Percentage of high-suitable area in the province (%)	Percentage of high-suitable area in China (%)
Tibet	0.00	0.00	0.44	122.84	/	/
Henan	0.00	0.00	0.78	16.70	/	/
Jiangsu	0.00	0.00	4.57	10.72	/	/
Anhui	0.00	0.00	8.14	14.01	/	/
Sichuan	0.00	0.11	4.06	48.60	/	/
Hubei	0.00	0.05	7.81	18.59	/	/
Chongqing	0.00	0.00	3.87	8.24	/	/
Shanghai	0.00	0.18	0.40	0.63	/	/
Zhejiang	0.90	1.72	6.77	10.55	8.0	9.9
Hunan	0.00	6.01	12.15	21.18	/	/
Jiangxi	0.00	0.77	14.40	16.69	/	/
Yunnan	0.02	0.82	17.49	39.41	0.1	0.2
Guizhou	0.00	0.00	5.99	17.62	/	/
Fujian	1.30	2.85	6.70	12.40	10.5	14.3
Guangxi	0.59	8.51	11.52	23.76	2.4	6.5
Taiwan	0.56	0.64	1.12	3.60	15.6	6.1
Guangdong	3.06	8.36	4.14	17.97	17.0	33.6
Hong Kong	0.00	0.09	0.00	0.11	/	/
Hainan	2.69	0.2	0.02	3.54	76.0	29.5
China	9.12	30.31	110.37	/	/	1.0

[a]Indicates the total area of the corresponding province.

coincides with the actual distribution of RPW, indicating that the MaxEnt prediction has some reference value.

As global warming continues, the area of distribution of RPW in low and high suitable habitat is likely to increase further, although the extent of variation in low and high suitable habitat for the insect varies under different climate scenarios. Fortunately, the overall distribution of RPW will continue to be concentrated in the southern regions without significant expansion towards the north. However, there is a more noticeable trend towards an increase in the proportion of high suitable areas in each province. There are many factors that influence the geographical distribution of species, and climate is among the most important. The key environmental variables affecting the distribution, namely BIO 1, BIO 2, BIO 6, BIO 16 and BIO 17, were screened based on the insect's contribution to the probability of occurrence, with BIO 1 having the greatest impact on the distribution; and the dividing line between the unsuitable areas and the low, medium and high suitable habitat areas mentioned above, as a whole, roughly coincides with the Qinling-Huaihe River line. This line is the 0°C isotherm in January in China, and also the demarcation line between the warm temperate zone and the subtropical zone (Xu *et al.*, 2021). This suggests that temperature may be a more important factor limiting the distribution of RPW in climatic conditions. BIO 1 represents the annual mean temperature. RPW demonstrates a higher suitability within the range of 24.6–29.4°C. However, the annual mean temperature in China typically ranges

between 10 and 15°C (Chaoli *et al.*, 2023), indicating that the preferred temperature range of the insect exceeds the country's average. This is also one of the reasons why the RPW is not distributed in most parts of China. However, Hainan Province has the largest distribution of RPW. This province falls under a tropical monsoon climate, with an annual average temperature ranging from approximately 25 to 28°C (Xinyue *et al.*, 2023), which creates favourable conditions for the survival of RPW. It is worth emphasising that in northern China, during the coldest months, the lowest temperature can drop to as low as −20°C or even lower (Yu *et al.*, 2023). Due to the generally colder climate characteristics in the north, RPW tends to be concentrated in the southern regions. In China, the diurnal temperature variation decreases from northeast to southwest (Kebiao *et al.*, 2023). Based on the preference of this pest for diurnal temperature variation, a range of 2.80–5.50°C is considered suitable. Overall, RPW tends to favour environments with small diurnal temperature variations. The southern coastal regions of China happen to fall into this category. This coincides with the current concentrated distribution area, thus confirming the predictions of this study.

Based on the previous description of the harmful potential of RPW pests, the prevention and control of this insect are particularly important. In the final analysis, the future distribution prediction of RPW in this paper also aims to provide a reliable reference for better control of the insect as well as future control efforts in terms of geographic distribution. For farmers, more convenient chemical control is preferred when dealing with pest

Table 3. Prediction of the suitable areas for *R. ferrugineus* under current and future climatic conditions

Decade	Scenarios	Predicted area (10⁴ km²)			Comparison with current distribution (%)		
		High-suitable area	Moderate-suitable area	Low-suitable area	High-suitable area	Moderate-suitable area	Low-suitable area
Current		9.11	30.31	110.38			
2050s	SSP1-2.6	8.90	34.00	121.09	−2.3	12.2	9.7
	SSP2-4.5	8.66	28.58	121.34	−4.9	−5.7	9.9
	SSP5-8.5	13.51	22.93	152.42	48.3	−24.3	38.1
2090s	SSP1-2.6	7.51	32.20	108.38	−17.6	6.2	−1.8
	SSP2-4.5	8.75	34.40	124.75	−4.0	13.5	13.0
	SSP5-8.5	11.05	27.57	129.68	21.3	−9.0	17.5

and disease problems. However, chemical control brings both the environmental pollution of pesticides, the resistance of RPW to pesticides and the health problems of workers, which cannot be avoided at present. In comparison, biological control appears to be safer. Some studies have shown that Entomopathogenic nematodes (EPNs) are an effective biocontrol agent against the insect. It can feed on and attack target pests without harming the environment and other non-target organisms. ENPs and their symbiotic bacteria have a reciprocal interaction that can kill the host in a short period of time and is a method of control worth considering (Nurashikin-Khairuddin *et al.*, 2022).

In this work, 19 bioclimatic variables were combined and modelled using the MaxEnt model to explore the geographic distribution of the RPW in China. At the same time, a hierarchical assessment of the insect's suitable distribution area was carried out. The 19 bioclimatic variables characterise the climate mainly in terms of indicators of both temperature and precipitation. Although it is already a relatively well-established indicator for climate, the survival of a species will also be affected by topography, terrain, elevation, species competition, human activities, etc. (Morales and Fernández, 2020). As a result, there are limitations in the breadth of data collection, and the predicted potentially suitable area will deviate somewhat from the actual suitable area (Convertino *et al.*, 2014). In future prediction efforts, additional research should obtain richer data as the modelling technology continues to mature and to expand the biotic and abiotic variables in the model to produce more accurate predictions. Although there is some room for improvement, this study successfully predicted the potential suitable distribution area of RPW within China based on the MaxEnt model with high reliability.
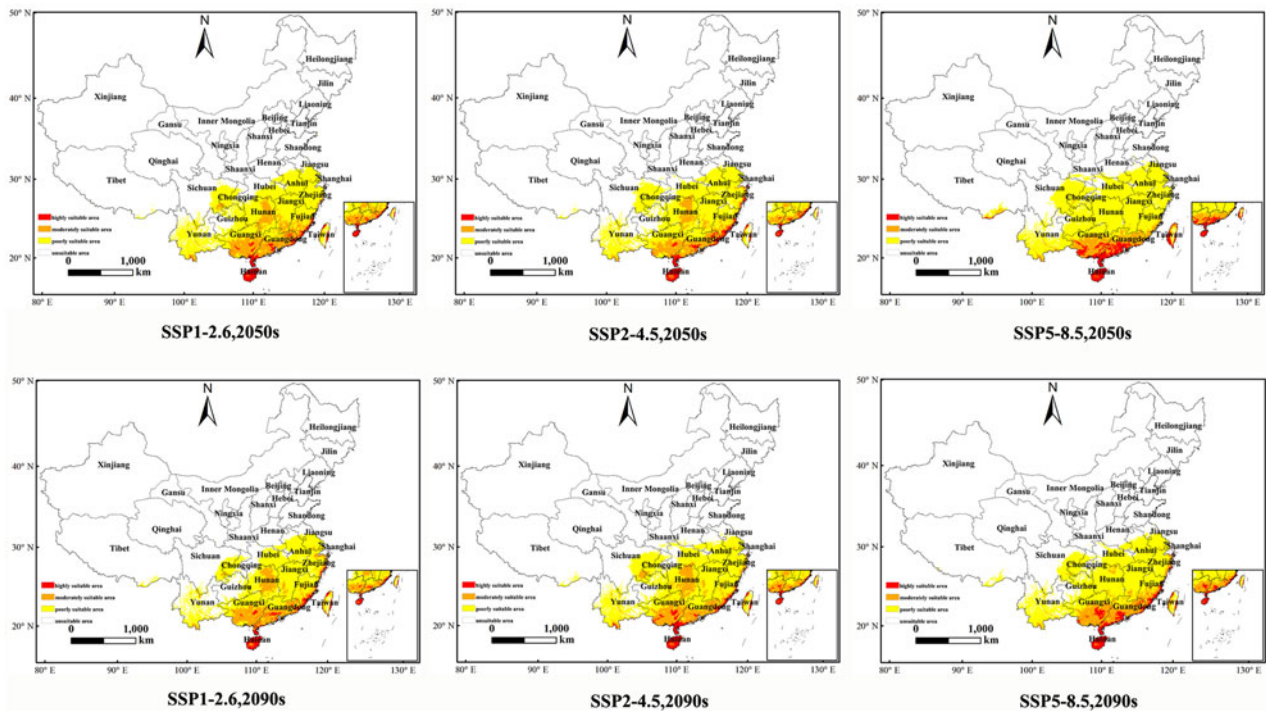

Figure 5. Potential distribution of suitable areas for *R. ferrugineus* based on different climate change scenarios in China. The probability of *R. ferrugineus* is shown by the colour scale in the area. Red indicates a highly suitable area with a probability higher than 0.66, orange indicates a moderately suitable area with a probability of 0.33–0.66, yellow indicates a poorly suitable area with a probability ranging from 0.05 to 0.33, and white represents unsuitable areas.

Conclusion

In this study, the potential geographic distribution areas of the RPW under three climate change scenarios (SSP1-2.6, SSP2-4.5 and SSP5-8.5) were successfully simulated based on the MaxEnt model for the current and two future periods (2050s and 2090s). Under the current climatic conditions, these southeastern coastal areas, such as Hainan, Guangdong, Fujian, Guangxi and Taiwan, are the main regions of the high suitability zones, which cover a total area of $9.12 \times 10^4 \, \text{km}^2$. The most significant factors (thresholds) affecting their distribution were temperature followed by precipitation, including annual mean temperature (24.6–29.4°C), mean diurnal range (2.80–5.50°C), minimum temperature of coldest month (15.8–23.2°C), precipitation of wettest quarter (=755 mm) and precipitation of driest quarter (=80 mm). The predicted potentially suitable distribution areas for RPW are in excellent agreement with actual occurrences. In order to more accurately model changes in the suitable geographic distribution of the pest under future climate change scenarios and to better control the pest, the combined effects of biotic and abiotic factors need to be fully considered in future research. This work aims to provide some theoretical references for the prediction and forecasting work of RPW as well as in the area of pest and disease control.

References

Abdel-Raheem MA, ALghamdi HA and Reyad NF (2019) Virulence of fungal spores and silver nano-particles from entomopathogenic fungi on the red palm weevil, *Rhynchophorus ferrugineus* Olivier (Coleoptera: Curculionidae). *Egyptian Journal of Biological Pest Control* **29**, 97. doi: 10.1186/s41938-019-0200-2

Abdel Raheem M, ALghamdi HA and Reyad NF (2020) Nano essential oils against the red palm weevil, *Rhynchophorus ferrugineus* Olivier (Coleoptera: Curculionidae). *Entomological Research* **50**, 215–220. doi: 10.1111/1748-5967.12428

Abdelsalam S, Alzahrani AM, Elmenshawy OM and Abdel-Moneim AM (2020) Antioxidant status and ultrastructural defects in the ovaries of red palmweevils (*Rhynchophorus ferrugineus*) intoxicated with spinosad. *Entomological Research* **50**, 309–316.

Ahmadi M, Hemami MR, Kaboli M and Shabani F (2023) MaxEnt brings comparable results when the input data are being completed; model parameterization of four species distribution models. *Ecology and Evolution* **13**, e9827. doi: 10.1002/ece3.9827

Ahmed R and Freed S (2021) Virulence of *Beauveria bassiana* Balsamo to red palm weevil, *Rhynchophorus ferrugineus* (Olivier) (Coleoptera: Curculionidae). *Egyptian Journal of Biological Pest Control* **31**, 1–4. doi: 10.1186/s41938-021-00422-5

Alsamadisi AG, Tran LT and Papeş M (2020) Employing inferences across scales: integrating spatial data with different resolutions to enhance Maxent models. *Ecological Modelling* **415**, 108857. doi: 10.1016/j.ecolmodel.2019.108857

Alshammari N, Alazmi M, Alanazi NA, Sulieman AE, Veettil VN and Ponce-Alonso M (2022) A comparative study on the microbial communities of *Rhynchophorus ferrugineus* (red palm weevil)-infected and healthy palm trees. *Arabian Journal for Science and Engineering* **47**, 6735–6746. doi: 10.1007/s13369-021-05979-9

Barber RA, Ball SG, Morris RKA and Gilbert F (2022) Target-group backgrounds prove effective at correcting sampling bias in Maxent models. *Diversity and Distributions* **28**, 128–141. doi: 10.1111/ddi.13442

Booth TH, Nix HA, Busby JR and Hutchinson MF (2014) *et al.* bioclim: the first species distribution modelling package, its early applications and relevance to most currentMaxEnt studies. *Diversity and Distributions* **20**, 1–9. doi: 10.1111/ddi.12144

Bowler MG (2014) Species abundance distributions, statistical mechanics and the priors of MaxEnt. *Theoretical Population Biology* **92**, 69–77. doi: 10.1016/j.tpb.2013.12.002

Chaoli T, Yidong Z, Heli W and Yuanyuan W (2023) Temporal and spatial variation characteristics of tropopause temperature over China in recent 40 years. *Journal of Atmospheric and Environmental Optics* **18**, 25–35. doi: 10.3969/j.issn.1673-6141.2023.01.003

Convertino M, Muñoz-Carpena R, Chu-Agor ML, Kiker GA and Linkov I (2014) Untangling drivers of species distributions: global sensitivity and uncertainty analyses of MaxEnt. *Environmental Modelling & Software* **51**, 296–309. doi: 10.1016/j.envsoft.2013.10.001

Costa H, Ponte NB, Azevedo EB and Gil A (2015) Fuzzy set theory for predicting the potential distribution and cost-effective monitoring of invasive species. *Ecological Modelling* **316**, 122–132. doi: 10.1016/j.ecolmodel.2015.07.034

El-Zoghby IRM, Awad NS, Alkhaibari AM and Abdel-Hameid NF (2022) Ultrastructure traits and genetic variability of red palm weevil *Rhynchophorus ferrugineus* (Olivier) adults from different geographical locations in Egypt. *Diversity* **14**, 404. doi: 10.3390/d14050404

Fiaboe M and Peterson KK (2012) Predicting the potential worldwide distribution of the red palm weevil *Rhynchophorus ferrugineus* (Olivier) (Coleoptera: Curculionidae) using ecological niche modeling. *Florida Entomologist* **95**, 659. doi: 10.1653/024.095.0317

Fourcade Y, Engler JO, Rodder D and Secondi J (2014) Mapping species distributions with MAXENT using a geographically biased sample of presence data: a performance assessment of methods for correcting sampling bias. *PLoS ONE* **9**, e97122. doi: 10.1371/journal.pone.0097122

Fredriksen HB, Smith CJ, Modak A and Rugenstein M (2023) 21st Century scenario forcing increases more for CMIP6 than CMIP5 models. *Geophysical Research Letters* **50**, e2023GL102916. doi: 10.1029/2023GL102916

Gao R, Liu L, Zhao L and Cui S (2023) Potentially suitable geographical area for *Monochamus alternatus* under current and future climatic scenarios based on optimized MaxEnt model. *Insects* **14**, 182. doi: 10.3390/insects14020182

Ge X, He S, Wang T, Yan W and Zong S (2015) Potential distribution predicted for *Rhynchophorus ferrugineus* in China under different climate warming scenarios. *PLoS ONE* **10**, e0141111. doi: 10.1371/journal.pone.0141111

Guillera-Arroita G, Lahoz-Monfort JJ, Elith J (2014) Maxent is not a presence-absence method: a comment on Thibaud *et al. Methods in Ecology and Evolution* 5, 1192–1197. doi: 10.1111/2041-210X.12252

Halvorsen R, Mazzoni S, Dirksen JW, Næsset E, Gobakken T and Ohlson M (2016) How important are choice of model selection method and spatial autocorrelation of presence data for distribution modelling by MaxEnt? *Ecological Modelling* 328, 108–118. doi: 10.1016/j.ecolmodel.2016.02.021

Harte J, Umemura K and Brush M (2021) DynaMETE: a hybrid MaxEnt-plus-mechanism theory of dynamic macroecology. *Ecology Letters* 24, 935–949. doi: 10.1111/ele.13714

Kebiao M, Yibo Y, Bing Z, Zijin Y and Mengmeng C (2023) Surface temperature analysis of temporal and spatial changes and driving factors in China. *Journal of Catastrophology* 38, 60–73. doi: 10.3969/j.issn.1000-811X.2023.02.010

Korbel J (2021) Calibration invariance of the MaxEnt distribution in the maximum entropy principle. *Entropy-Switz* 23, 96. doi: 10.3390/e23010096

Kramer-Schadt S, Niedballa J and Pilgrim JD (2013) The importance of correcting for sampling bias in MaxEnt species distribution models. *Diversity and Distributions* 19, 1366–1379. doi: 10.1111/ddi.12096

Kurdi H, Al-Aldawsari A, Al-Turaiki I and Aldawood AS (2021) Early detection of red palm weevil, *Rhynchophorus ferrugineus* (Olivier), infestation using data mining. *Plants-Basel* 10, 95. doi: 10.3390/plants10010095

Lijiao P and Yihang L (2022) Survey on the occurrence of red and brown weevil in Chenggong District, Kunming and its prevention and control measures. *Hubei Plant Protection* 190, 54–55.

Losada M, Penas VA, Holik F and Lamberti PW (2022) MaxEnt principle and reduced density matrix estimation. *Physica A: Statistical Mechanics and its Applications* 600, 127517. doi: 10.1016/j.physa.2022.127517

Montiel EE, Mora P, Rico-Porras JM, Palomeque T and Lorite P (2022) Satellitome of the red palm weevil, *Rhynchophorus ferrugineus* (Coleoptera: Curculionidae), the most diverse among insects. *Frontiers in Ecology and Evolution* 10, 826808. doi: 10.3389/fevo.2022.826808

Morales NS and Fernández IC (2020) Land-cover classification using MaxEnt: can we trust in model quality metrics for estimating classification accuracy? *Entropy-Switz* 22, 342. doi: 10.3390/e22030342

Nengjie Q (2022) The application of palm plants in Maoming urban landscape. *Anhui Agricultural Science* 50, 127–129.

Nurashikin-Khairuddin W, Abdul-Hamid SNA, Mansor MS, Bharudin L, Othman Z and Jalinas J (2022) A review of entomopathogenic Nematodes as a biological control agent for red palm weevil, *Rhynchophorus ferrugineus* (Coleoptera: Curculionidae). *Insects* 13, 245. doi: 10.3390/insects13030245

Wang X, Hou W, Song C, Deng MH, Li Y and Wang JQ (2021) BW-MaxEnt: a novel MCDM method for limited knowledge. *Mathematics-Basel* 9, 1587. doi: 10.3390/math9141587

Wang Z, Xu D, Liao W, Xu Y and Zhuo Z (2023) Predicting the current and future distributions of *Frankliniella occidentalis* (Pergande) based on the MaxEnt species distribution model. *Insects* 14, 458. doi: 10.3390/insects14050458

West AM, Kumar S, Brown CS, Stohlgren T and Bromberg J (2016) Field validation of an invasive species Maxent model. *Ecological informatics* 36, 126–134. doi: 10.1016/j.ecoinf.2016.11.001

Xinyue H, Mingjin J and Buda S (2023) Trends of summer apparent temperature in China metropolises for 1961–2022. *Energy Research and Management* 15, 106–113.

Xu L, Qu J, Han J, Zeng J and Li H (2021) Distribution and evolutionary in household energy-related CO2 emissions (HCEs) based on Chinese north–south demarcation. *Energy Reports* 7, 6973–6982. doi: 10.1016/j.egyr.2021.09.104

Yang T, Wu L, Liao C, Li D, Young Shin T and Nai YS (2023) Entomopathogenic fungi-mediated biological control of the red palm weevil *Rhynchophorus ferrugineus. Journal of Asia-Pacific Entomology* 26, 102037. doi: 10.1016/j.aspen.2023.102037

Yasin M, Wakil W and Qayyum MA (2021) Biocontrol potential of entomopathogenic fungi, nematodes and bacteria against *Rhynchophorus ferrugineus* (Olivier). *Egyptian Journal of Biological Pest Control* 31, 138. doi: 10.1186/s41938-021-00484-5

Yu LH, Xianjie M, Jiahui T and Chunhan J (2023) Characterization of temperature changes in the arid zone of Northwest China in the past millennium and analysis of their causes. *Quaternary Sciences* 43, 1089–1100.

Zhang H, Bai J and Huang S (2020) Neuropeptides and G-protein coupled receptors (GPCRs) in the red palm weevil *Rhynchophorus ferrugineus* Olivier (Coleoptera: Dryophthoridae). *Frontiers in Physiology* 11, 159. doi: 10.3389/fphys.2020.00159

Zhijun S (1998) Rihuazi and <the Rihuazi Materia Medica>. *Jiangsu Traditional Chinese Medicine* 12, 3–5.

Zhou Y, Zhang Z and Zhu B (2021) MaxEnt modeling based on CMIP6 models to project potential suitable zones for *Cunninghamia lanceolata* in China. *Forests* 12, 752. doi: 10.3390/f12060752

Zhu J, Li J and Wang C (2019) Anatomy of the windmill palm (*Trachycarpus fortunei*) and its application potential. *Forests* 10, 1130. doi: 10.3390/f10121130